

## Research Article

# Characterization and Application of the Thermal Neutron Radiography Beam in the Egyptian Second Experimental and Training Research Reactor (ETRR-2)

M. A. Abou Mandour, R. M. Megahid, M. H. Hassan, and T. M. Abd El Salam

Received 25 March 2007; Revised 24 October 2007; Accepted 22 November 2007

Recommended by Piero Ravetto

The Experimental, Training, Research Reactor (ETRR-2) is an open-pool multipurpose reactor (MPR) with a core power of 22 MW<sub>th</sub> cooled and moderated by light water and reflected with beryllium. It has four neutron beams and a thermal column as the main experimental devices. The neutron radiography facility unit utilizes one of the radial beam tubes. The track-etch technique using nitrocellulose films and converter screen is applied. In this work, the radial neutron beam for the thermal neutron radiography facility has been characterized and the following values were determined: thermal flux of  $1.5 \times 10^7$  n/cm<sup>2</sup> · s,  $n_{th}/\gamma$  ratio of  $0.1 \times 10^6$  n · cm<sup>-2</sup> · mR<sup>-1</sup>; a Cd ratio of 10.26, a resolution of 0.188 mm, and L/D ratio of 117.3. This characterization verifies the design parameters of the unit. Various radiographs were taken and results indicate that the neutron radiography facility of the ETRR-2 holds promising opportunities for nuclear as well as nonnuclear applications.

Copyright © 2007 M. A. Abou Mandour et al. This is an open access article distributed under the Creative Commons Attribution License, which permits unrestricted use, distribution, and reproduction in any medium, provided the original work is properly cited.

## 1. INTRODUCTION

The Experimental, Training, Research Reactor (ETRR-2) is a multipurpose reactor (MPR) [1–3]. It is a pool-type reactor with an open water surface and variable core arrangement. The core power is 22 MW<sub>th</sub> cooled by light water, moderated by water and with beryllium reflectors. Figure 1 shows a schematic of the MPR core internals and beam tubes.

The MPR reactor has four neutron beams and a thermal column as the main experimental devices. As shown in Figure 2, the four neutron beams tubes are

- (1) the neutron radiography facility (NRF);
- (2) the radial beam tube;
- (3) the tangential beam tube;
- (4) the underwater neutron radiography facility (UNRF).

## 2. THE ETRR-2 NEUTRON RADIOGRAPHY FACILITY

The neutron radiography facility comprises the following subsystems.

### (1) The irradiation conduit (collimator)

It is submerged into the water of the reactor tank. It consists of a divergent aluminum tube lined by a two-millimeter cad-

mium sheet. The collimator is placed completely inside the reactor tank. The collimator inlet has a diameter of 30 mm. As shown in Figure 3, a revolving system allows turning the collimator between two positions: the working position (horizontal) and the resting position (vertical). The revolving system is operated by means of the remote control. A gamma-ray filter is placed at the inlet of the beam. It is separated from the beryllium reflector (which is placed in one row around the core) by a two-millimeter water gap. The gamma filter is made of lead, and has a thickness of 145 millimeters.

### (2) The irradiation channel

It cuts across the concrete shielding. The channel is surrounded by a lead annulus; and both are submerged into the biological shield. The main functions of the irradiation channel are as follows: to provide the necessary shielding to both neutron and gamma rays when it is flooded with water, that is, when the facility is not operating; and to contribute to the collimation of neutrons because it is the continuation of the collimator when it is dried and filled with nitrogen. The biological shielding is composed of heavy and ordinary concrete.

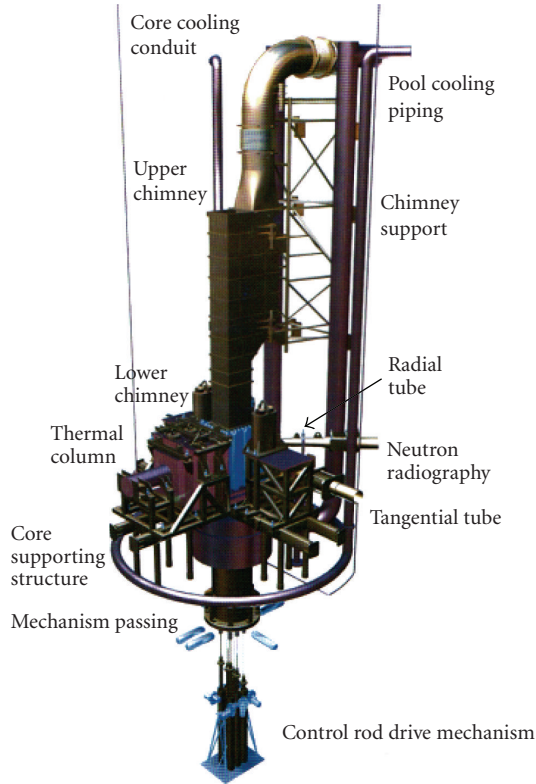


FIGURE 1: MPR core internals and beam tubes.

### (3) The beam channel port (shutter)

It is a movable metallic box filled with lead, telecommanded by a servomechanism that controls the movement when shifting between the *open* or exposure position and the *closed* position. It has a thickness of 20 cm. The main purpose of the beam channel port is to provide complementary biological shielding to allow personnel to enter into the neutron radiography room.

### (4) The sample holder

It is a movable table placed in front of the beam channel port. It allows the positioning of samples to be irradiated by regulating the movement either vertically or horizontally and also rotationally around its vertical axis in order to expose different shapes and sizes of samples, which can be placed either from within the cell (explained below) or from the outside. When placing samples from outside the cell, the cassette-holder carriage must be used as explained below.

### (5) The cassette-holding device

It fastens the sensitive film and allows introducing and extracting it to/from the cell without having to enter into it. The device consists of a rail that goes from a radiological secure position (outside the room) to the irradiation port (inside the room). Hanging from it, a transport carriage can slide from outside to inside the room. It is manually operated with

a crank from outside the room where the operator is in a radiological safe position.

### (6) The beam catcher

It is a movable shielding, placed behind the sample holder, designed to incorporate light and heavy elements, and high-neutron absorption cross-section materials. Its function is to moderate fast and epithermal neutrons, to absorb thermal neutrons, and to attenuate resultant capture gamma rays as required. The beam catcher has been provided with wheels so as to facilitate its positioning. It has a supporting metallic structure, a borate polyethylene head, a concrete block, and a lead disc at the far end. The use of lead clad cover is to shield secondary and scattered gamma radiation from the beam catcher.

### (7) The cell

It takes care of the back-scattered thermal neutrons. The cell is a concrete structure serving to shield the working area around the irradiation facility. It has a labyrinth-wall arrangement in order to provide an adequate accessibility for operating personnel.

The facility applies the track-etch technique using nitrocellulose films and converter screen. The combination of a nitrocellulose film and a lithium or boron converter screen provides a direct imaging method. Usually converters are applied in front and behind the film. In this technique,  $\alpha$  particles are emitted by the converter screen in response to incoming neutrons. The  $\alpha$  particles produce an image in the nitrocellulose film by creation of small defects (tracks), which are enhanced and made visible by an etching process. Etching is performed in hot sodium hydroxide solution (e.g., in 10% NaOH for 20 minutes at 600°C). It is important to note that the nitrocellulose films are insensitive to gamma radiation.

## 3. DESIGN PARAMETERS OF NEUTRON RADIOGRAPHY FACILITY [4, 5]

Proper utilization of the neutron radiography facility necessitates performing flux mapping as well as determination of certain parameters such as  $n_{th}/\gamma$  ratio, Cd ratio, the L/D ratio, as well as the image resolution. This is explained in the following section.

The desirable features of a thermal neutron beam for neutron radiographic applications would include the following [4, 5].

### (1) High thermal neutron intensity

This should be of the order of  $10^6$   $n/cm^2 \cdot s$  or higher. This is mainly to obtain results in a reasonable time.

### (2) Low gamma radiation intensity

The intensity of gamma radiation in the beam affects the amount of biological shielding required, determines whether or not direct-method neutron radiography is possible, and

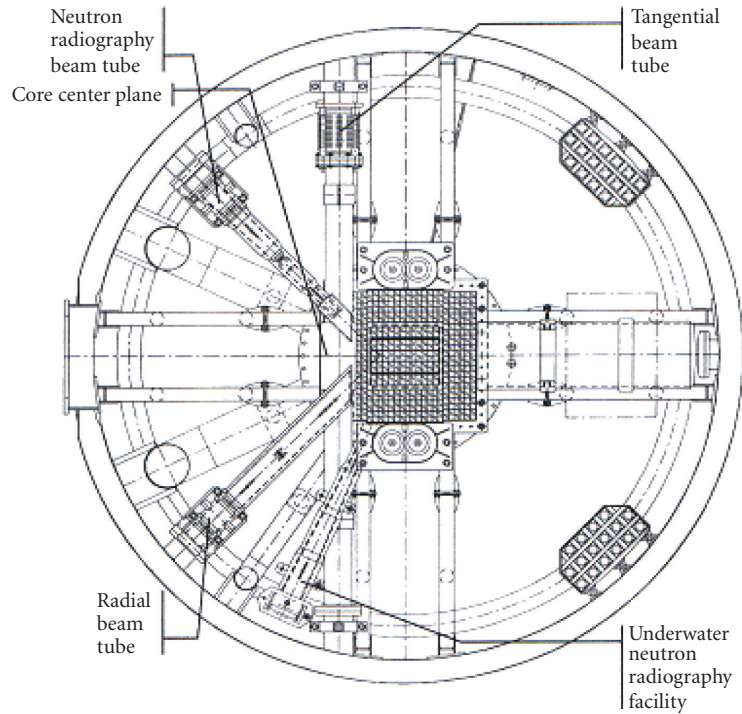


FIGURE 2: MPR beam tubes.

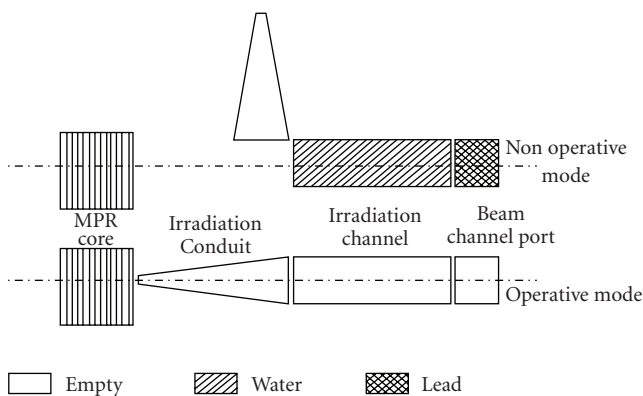


FIGURE 3: Normal states of the neutron radiography facility.

influences the quality of generated neutron radiographs. Radiographically, the absolute intensity of gamma radiation is less important than is the relative contribution of gamma rays to the generation of the image as compared to the contribution from neutrons. Thus, the ratio of the thermal neutron intensity in  $n/cm^2 \cdot s$  to the gamma radiation intensity in mR/sec (i.e.,  $n_{th}/\gamma$  ratio) needs to be  $10^6$  or higher. This condition ensures that gamma-ray contribution to the generation of the image will be small relative to that from neutrons.

*(3) Relatively low-fast-neutron intensity*

This is due to the fact that, generally speaking, neutrons of higher energy than thermal neutrons will give greater penetration but with more scattering due to object and shield-

ing scattering, so producing poorer images (i.e., less contrast). The relatively low-fast-neutron intensity is measured by the value of the Cd ratio. This is defined as the ratio of the response of two identical neutron detectors, usually activation types such as indium or gold, one exposed bare to the beam while the other is cadmium-covered during exposure. The cadmium covered detector records primarily neutrons having energy above the cadmium cutoff energy; that is, 0.5 eV; and the ratio is a measure of thermalization in the neutron spectrum. Good design criteria require the Cd ratio to be greater than 10.

*(4) Large area coverage for the neutron beam*

This is needed in order that large objects can be radiographed using as few exposures as possible.

*(5) Low angular divergence*

This is in order that resolution capabilities for thicker objects can be good. If the neutron beam diverges very rapidly to a large size, then the outer portion of the images produced will suffer significant distortion. Conversely, if the beam is very long or if the image size is small, then the outer portion of the image will be less distorted. Beam divergence is judged by the L/D ratio. This is defined as the distance between the entrance aperture to the image plane divided by the neutron aperture diameter. As L/D is increased, the image definition will be improved.

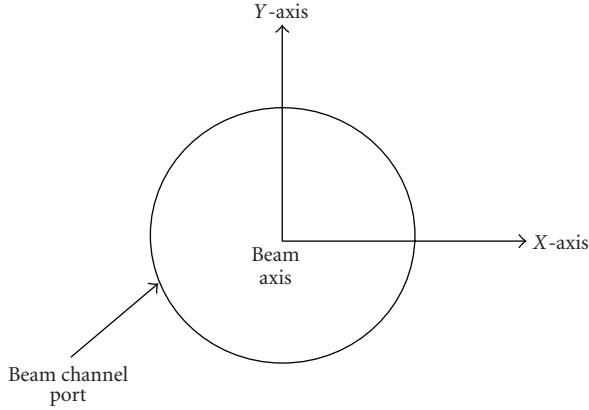


FIGURE 4: Geometrical arrangement during the flux mapping process.

## 4. CHARACTERIZATION OF THE ETRR-2 NEUTRON RADIOGRAPHY BEAM

### 4.1. Flux mapping

Flux mapping at the beam opening was determined using the conventional gold sample technique. Bare and cadmium-covered gold samples were placed at  $X$ - and  $Y$ -axes as shown in Figure 4. Each axis was divided into three points, distanced 4, 8, 12 cm apart from the beam axis. Samples were irradiated for 4 hours, at  $13.3 \text{ MW}_{\text{th}}$ . The high exposure time ensures proper evaluation of the flux values. After 102 hours, which is the time needed for the short-lived radionuclides to decay, the  $\gamma$ -ray spectra of the activated gold samples were measured using a typical high-resolution  $\gamma$ -spectrometer based on a shielded HPGe-detector, coaxial type, with  $133 \text{ cm}^3$  effective volume, 30% photopeak relative efficiency, and energy resolution of 1.95 keV FWHM for the 1332 keV  $\gamma$ -ray line of  $^{60}\text{Co}$ .

Flux values determined from the bare gold foils give the total flux while flux values determined from the Cd-covered gold samples give the flux above the Cd cutoff energy. The difference between the two values gives the thermal flux as related to the thermal neutron radiography technique. Figures 5 and 6 show the spatial variation of the thermal neutron flux along the  $X$ - and  $Y$ -axes. It is important to note that the beam channel port is 30 cm in diameter. As we move along the beam axis towards the reactor core (directly after the beam channel port as shown in Figure 3), the beam channel radius is 22 cm. Thus, during the flux mapping measurements, the flux decreases sharply at 12 cm away from the beam axis and its value was not reported in the figures.

The maximum uncertainty in determining the flux was 5.6%. Uncertainty is attributed to gold-sample-weight determination, detector system counting statistics, and nuclear data evaluation. Along the  $X$ -axis, uncertainty in the flux measurement ranges from 4.5% at  $x = 0$  to a maximum of 5.6 at  $x = -8$  cm away from the beam axis. Along the  $Y$ -axis, uncertainty in the flux measurement ranges from 4.5% at  $y = 0$  to a maximum of 5.2% at  $y = 8$  cm away from the beam

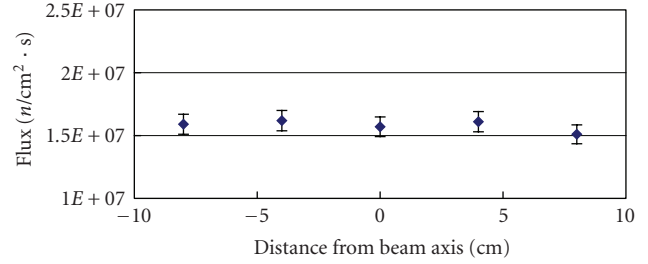


FIGURE 5: Thermal neutron flux mapping along the  $X$ -axis.

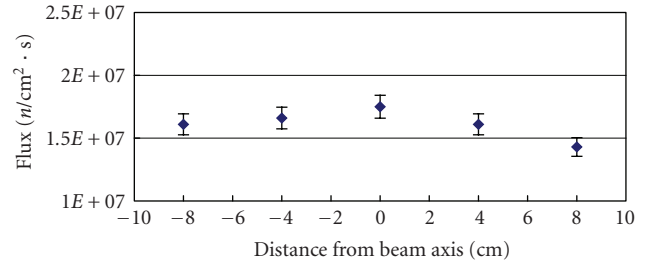


FIGURE 6: Thermal neutron flux mapping along the  $Y$ -axis.

axis. From Figures 5 and 6, it is obvious that the flux is nearly symmetric around the beam axis.

### 4.2. Determination of the Cd Ratio

The Cd ratio is defined as

$$\text{Cd ratio} = A_{\text{bare}}/A_{\text{covered}}, \quad (1)$$

where  $A_{\text{bare}}$  is the activity of bare golden sample and  $A_{\text{covered}}$  is the activity of cadmium-covered sample.

During the flux mapping calculations, both bare and covered activity values were determined following the geometrical arrangement shown in Figure 4. Thus, Figures 7 and 8 show the spatial variation of the Cd ratio. The Cd ratio ranges between  $9.33 \pm 5\%$  to  $11.19 \pm 5.2\%$ . Since the good quality neutron beam design criteria required the Cd ratio to be greater than 10, the measured Cd ratio is acceptable. However, this value indicates relatively high-neutron intensity above the Cd cutoff energy in the beam. Thus, if dynamic system neutron radiography would be applied in the facility, effects of neutron scattering would need to be taken into consideration to properly interpret the obtained images.

### 4.3. Determination of $n_{\text{th}}/\gamma$ ratio

Bare and cadmium-covered gold foils were irradiated for one hour at the beam center line directly facing the beam channel port; and the thermal neutron flux was measured as was done in the flux mapping process. The exposure rate was measured by an electronic dosimeter FH 41D-3 placed in the irradiation field for the same time and at the same point of the gold samples.

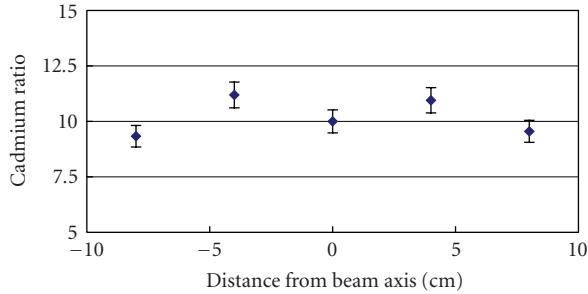


FIGURE 7: Variation of the Cd ratio along the X-axis.

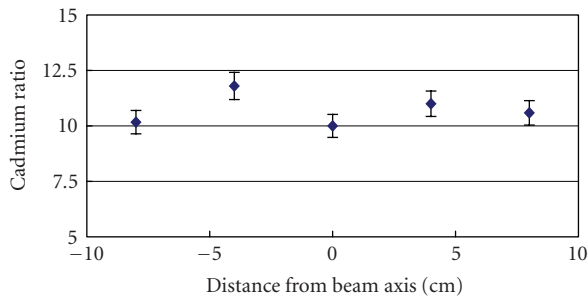


FIGURE 8: Variation of the Cd ratio along the Y-axis.

The thermal neutron flux was  $1.5 \times 10^7 \pm 4.5\% n/cm^2 \cdot s$  and the exposure rate was  $3.3 \pm 10\% Sv/hr$ , or  $3.3 \times 10^2 \pm 10\% R/hr$ . Since measurements were done for one hour, the exposure is taken to be  $3.3 \times 10^2 R$ . Thus,

$$n_{th}/\gamma = 0.1 \times 10^6 \pm 2\% n \cdot cm^{-2} \cdot mR^{-1}. \quad (2)$$

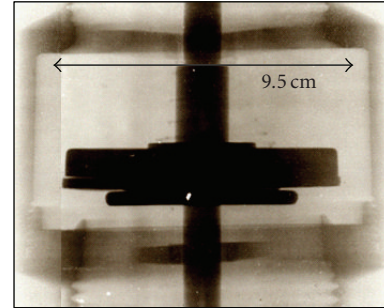
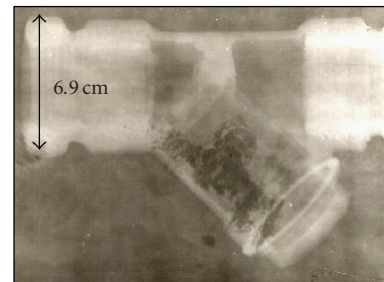
This value does not meet the good quality neutron beam design criteria, which specifies the ( $n/\gamma$ ) ratio to be  $>10^6 n/cm^2 \cdot mR$ . As mentioned before, the plastic nitrocellulose film used for imaging is insensitive to gamma rays. Thus, in light of the imaging method used, the characteristic  $n_{th}/\gamma$  is acceptable. However, a change in the beam design needs to be performed if other imaging techniques that are sensitive to gamma radiation are used.

#### 4.4. L/D ratio

Since the neutron entrance aperture diameter ( $D$ ) is 30 mm and the distance between the entrance aperture to the image plane ( $L$ ) is 351.8 cm, the L/D ratio is 117.3.

#### 4.5. Image resolution

This is usually done by reporting the smallest dimension that could be observed. Two samples (antimony and stainless steel) were used for resolution determination. During the commissioning phase of the radiography facility, the resolution was determined to be 1 mm by using KODAK film CA-80-15 type B. During the startup phase of the facility, after adjusting the exposure and etching times, further measure-

FIGURE 9: Defective copper nonreturn valve. (20 MW<sub>th</sub>, exposure time: 35 minutes; film type: CN85 type B; converter screen: BN1; etching time: 20 minutes).FIGURE 10: Defective Y filter with clear corrosion products in the drain part. (15 MW<sub>th</sub>, exposure time: 60 minutes; film type: LR115 type 1B; converter screen: BN1; etching time: 25 minutes).

ments were made. Experience showed that longer exposure times required less etching time.

Using CN 85 film type B and BN1 converter screen for irradiation time, 20 minutes, and etching time, 5 minutes, a copper wire of diameter 0.188 mm placed directly in front of the beam channel port could be observed.

## 5. TEST SAMPLES

Items related to the ETRR-2 operation like valves, detection probes, relays were imaged and analyzed. This includes a defective copper 2 in nonreturn valve, electronic relay, Y filter, electrical fuse, solenoid valve, different thickness of carbon steel, pocket and pen dosimeters, and gate valve. Representative radiographs are shown below.

Figure 9 represents a radiograph of a defected nonreturn valve made from copper. Due to the high-scattering cross-section of hydrogen, one can image plastic and/or rubber components housed in the valve heavy metal copper containment. Thus, the defect in the rubber gasket is quite obvious. The valve spring is slightly seen seated on the rubber gasket.

Figure 10 represents a radiograph of a defective Y filter. Corrosion deposits are obvious in the drain part of the filter.

Figure 11 shows a solenoid valve where the internal details are clear. Notice that the plastic cap hides the details of the upper parts of the valve (like the spring).

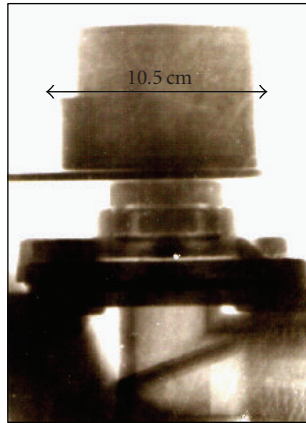


FIGURE 11: A solenoid valve with some internal details. (10.5 MW<sub>th</sub>, exposure time: 60 minutes; film type: LR115 type 1B; converter screen: BN1; etching time: 25 minutes).

## 6. CONCLUSIONS

The neutron beam for the neutron radiography facility of the ETRR-2, Egypt, has been characterized to have the following parameters: thermal flux of  $1.5 \times 10^7 \text{ n/cm}^2 \cdot \text{s}$ ,  $n_{\text{th}}/\gamma$  ratio of  $0.1 \times 10^6 \text{ n} \cdot \text{cm}^{-2} \cdot \text{mR}^{-1}$ ; a Cd ratio of 10.26, a resolution of 0.188 mm and L/D ratio of 117.3. This characterization verifies the design parameters of the unit. Various radiographs were taken; and results indicate that the neutron radiography facility of the ETRR-2 holds promising opportunities for nuclear as well as nonnuclear applications.

## ACKNOWLEDGMENT

The authors would like to acknowledge the cooperation of the involved staff of the ETRR-2.

## REFERENCES

- [1] I. D. Abdelrazek, M. K. Fayek, A. M. Shokr, and A. E. Ali, "General performance and utilization plan of egypt second research reactor," in *Proceedings of the 6th Meeting of the International Group on Research Reactors (IGORR '98)*, Taejon, Korea, April-May 1998.
- [2] M. K. Fayek and A. M. A. Shokr, "On the utilization of the ETRR2 neutron beams in research and applications," in *Proceeding of International Symposium on Research Reactors Utilization, Safety, and Management (IAEA '99)*, Lisbon, Portugal, September 1999.
- [3] [www.etr-2.aea.org.eg](http://www.etr-2.aea.org.eg).
- [4] J. C. Domanus, *Practical Neutron Radiography*, Kluwer Academic Publishers, Dordrecht, The Netherlands, 1992.
- [5] "Use of neutron beams for low and medium flux research reactors: radiography and material characterization," IAEA-TECDOC-837, IAEA October 1995.

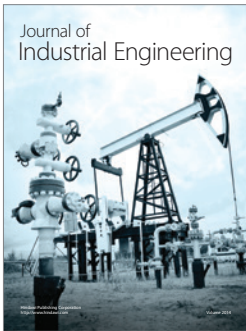
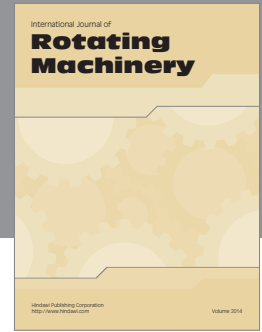
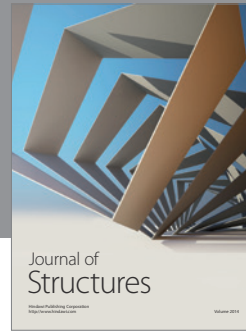
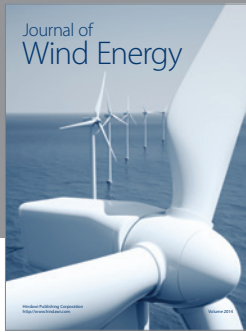
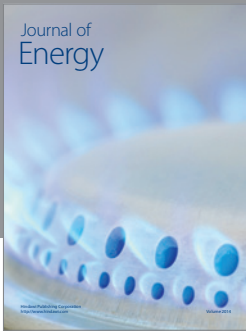
## AUTHOR CONTACT INFORMATION

**M. A. Abou Mandour:** Nuclear Engineering Department, Alexandria University, Alexandria 21544, Egypt; mohsenmandour@yahoo.com

**R. M. Megahid:** Atomic Energy Authority, P. O. Box 13975, Abu Zabal, Egypt; megahid@etr2-aea.org.eg

**M. H. Hassan:** Nuclear Engineering Department, Alexandria University, Alexandria 21544, Egypt; mhmheg@yahoo.com

**T. M. Abd El Salam:** Atomic Energy Authority, P. O. Box 13975, Abu Zabal, Egypt; tarek\_mongy@hotmail.com



**Hindawi**

Submit your manuscripts at  
<http://www.hindawi.com>

